SHORT REPORT

Slap restricts oncogenic Src-family kinase signaling to maintain colonic epithelial homeostasis

Dana Naim[1,2,3], Zouheir Houhou[1,2], Florent Cauchois[1,2], Kevin Espie[1,2], Valerie Simon[1], Yvan Boublik[1,2,3], Francina Langa Vives[4], Zeinab Homayed[5], Conception Paul[6], Morgan Maillard[7], Michael Hahne[6], Julie Pannequin[5], Julie Nguyen[1,2,3], Audrey Sirvent[1,2,3*†], Serge Roche[1,2,3*†]

[1]CRBM, Univ. Montpellier, CNRS, Montpellier, France; [2]Equipe labellisée FRM2023, CRBM, Univ. Montpellier, CNRS, Montpellier, France; [3]Equipe labellisée LIGUE2020, CRBM, Univ. Montpellier, CNRS, Montpellier, France; [4]Institut Pasteur, Mouse Genetics Engineering Center, Université Paris Cité, Paris, France; [5]IGF, Univ. Montpellier, CNRS, INSERM, Montpellier, France; [6]Equipe labellisée LIGUE2022, IGMM, Univ. Montpellier, CNRS, Montpellier, France; [7]IRCM, Univ. Montpellier, INSERM, Montpellier, France

***For correspondence:** audrey.sirvent@crbm.cnrs.fr (AS); serge.roche@crbm.cnrs.fr (SR)

[†]These authors contributed equally to this work

Competing interest: The authors declare that no competing interests exist.

Funding: See page 17

Preprint posted 05 January 2026
Sent for Review 13 January 2026
Reviewed preprint v1 31 March 2026
Reviewed preprint v2 05 August 2026
Version of Record 08 September 2026

Reviewing Editor: Frederic A Bard, Centre de Recherche en Cancérologie de Marseille, France

© Copyright Naim *et al*. This article is distributed under the terms of the Creative Commons Attribution License, which permits unrestricted use and redistribution provided that the original author and source are credited.

eLife Assessment

This is an **important** study on the role of Slap in restricting Src activity and proliferation of colonic cells in vivo. The authors present **solid** evidence that an EPHB2-SRC signaling axis stimulates the proliferation of colon precursors and is controlled by the Src-binding protein SLAP, whose loss promotes tumorigenesis.

Abstract Src-family kinases (SFKs) regulate proliferation in colonic epithelial cells (CECs), but the mechanisms that restrain their activity remain poorly defined. We identify Src-like adaptor protein (SLAP), a negative regulator of receptor tyrosine kinase signaling, as a key suppressor of SFK activity in the colon. Constitutive and inducible epithelial-specific Slap deletion using a villin-CreERT2 model increases CEC proliferation and accelerates tumorigenesis in the azoxymethane/dextran sodium sulfate model. Slap deficiency also enhances SFK-dependent expansion of normal and tumor-derived colonic organoids. Mechanistically, we identify the receptor tyrosine kinase EPHB2 as a critical upstream activator of SFKs and a direct target of SLAP-mediated regulation. Loss of Slap increased EphB2 protein abundance and tyrosine phosphorylation, and enhanced its association with active SRC. Pharmacological inhibition of EPHB2 suppressed SRC activation and reversed the hyperproliferative phenotype induced by Slap deficiency. Together, these findings uncover a non-genetic mechanism driving SFK activation during colonic transformation and establish SLAP as a tumor suppressor that constrains oncogenic EPHB2–SFK signaling in the colonic epithelium.

Introduction

The membrane-anchored tyrosine kinase (TK) SRC plays important roles in intestinal homeostasis and tumorigenesis. In particular, SRC and other members of its family (i.e. FYN and YES) drive intestinal stem/progenitor cell proliferation, tissue regeneration, and tumorigenesis in *Drosophila* and mouse models (***Cordero et al., 2014***; ***Imada et al., 2016***; ***Kohlmaier et al., 2015***; ***Sirvent et al., 2020***).

SRC is also an oncogene in human colorectal cancer (CRC). Aberrant SRC expression and activity in CRC (50% of CRC patients) is a marker of poor clinical prognosis, a promoter of therapeutic resistance, and a potent driver of metastasis (***Sirvent et al., 2012***; ***Summy and Gallick, 2003***; ***Yang et al., 2022***). This tumor activity is associated with cancer stem cell and epithelial-to-mesenchymal transition features. However, SRC is rarely mutated in CRC and the mechanisms underlying its oncogenic function remain elusive (***Irby et al., 1999***; ***Sirvent et al., 2012***; ***Summy and Gallick, 2003***). Consistently, SRC inhibitors developed for the clinic have failed in CRC due to ineffective signaling inhibition and inadequate patient selection (***Daud et al., 2012***; ***Parseghian et al., 2017***; ***Reddy et al., 2015***). Elucidating the mechanisms underlying this persistent signaling may reveal essential non-genetic mechanisms by which TKs promote tumorigenesis and allow the development of effective TK-based therapies in CRC.

During evolution, TK activities have come under the tight control of small adaptor proteins that exert negative regulatory functions (***Naudin et al., 2016***). The best example is the SOCS regulation of JAK/STAT inflammatory pathways. We discovered that SRC signaling is under the control of such an inhibitory mechanism through the membrane-anchored adaptor SLAP (Src-like adaptor protein), which displays high sequence homology with SRC N-terminus (***Manes et al., 2000***; ***Pandey et al., 1995***; ***Roche et al., 1998***; ***Sirvent et al., 2008***). Mechanistically, SLAP promotes degradation or prevents SRC binding to upstream receptors, resulting in inhibition of SRC signaling (***Dragone et al., 2006a***; ***Dragone et al., 2006b***; ***Kazi and Rönnstrand, 2012***; ***Myers et al., 2006***; ***Myers et al., 2005***; ***Roche et al., 1998***; ***Sirvent et al., 2008***; ***Wybenga-Groot and McGlade, 2015***). Slap-deficient mice revealed an essential function for this adaptor in controlling lymphocyte development and activation, where it is highly expressed (***Sosinowski et al., 2001***). We additionally reported an unsuspected tumor suppressor function of SLAP in CRC (***Naudin et al., 2014***). Notably, SLAP was found to be abundantly expressed in the intestinal epithelium. SLAP levels were reduced in 50% of CRC samples analyzed, and SLAP silencing in experimental CRC models promoted tumor formation and liver metastasis. Mechanistically, SLAP promotes degradation of SRC signaling RTK EPHA2 (***Naudin et al., 2014***) and destabilization of the mTORC2 complex, resulting in AKT signaling inhibition (***Dragone et al., 2006a***; ***Mevizou et al., 2026***). Although this observation suggests an important mechanism in the control of SRC function in the colon, genetic evidence for this mechanism is lacking. Here, we developed Slap-deficient mice models showing that Slap regulates SFK colonic epithelial function during homeostasis and tumorigenesis.

Results

Constitutive *Slap* inactivation increases CEC proliferation

To investigate SLAP function in the colon, we generated constitutive Slap-deficient mice by inserting a *LacZ* cassette into the *Slap* gene (*Slap-/-* mice) (***Figure 1A***). β-Galactosidase activity staining revealed a gradient of Slap expression toward the top of the crypts throughout the colonic epithelium (***Figure 1—figure supplement 1A***). This expression pattern was confirmed at the protein level by immunofluorescence staining using a Slap-specific antibody (***Figure 1A***). Loss of Slap led to increased colon thickness in 3-month-old mice, characterized by elongated crypts (***Figure 1A***). This epithelial hyperplasia was accompanied by elevated cell (CEC) proliferation (***Figure 1A***) and an increased number of goblet cells (***Figure 1—figure supplement 1B***), indicating that Slap regulates both CEC proliferation and differentiation.

RNAscope analysis of Lgr5, a marker of colonic epithelial stem cells (CSCs) (***Barker et al., 2007***), showed increased expression at crypt bases in Slap-deficient mice (***Figure 1A***), suggesting enhanced CSC traits. Given the role of SFKs in regulating colonic stem/progenitor proliferation (***Cordero et al., 2014***; ***Imada et al., 2016***; ***Kohlmaier et al., 2015***; ***Sirvent et al., 2020***), we assessed whether Slap modulates SFK activity. Immunohistochemical analysis of an antibody detecting the activated form of Src (pSRC), which also cross-reacts with other p-SFKs, revealed increased SFK activity throughout the crypts of Slap-deficient mice (***Figure 1—figure supplement 1B***). This suggests that SLAP plays a role in regulating intestinal epithelial homeostasis, in addition to its well-established function in lymphocyte development (***Sosinowski et al., 2001***).

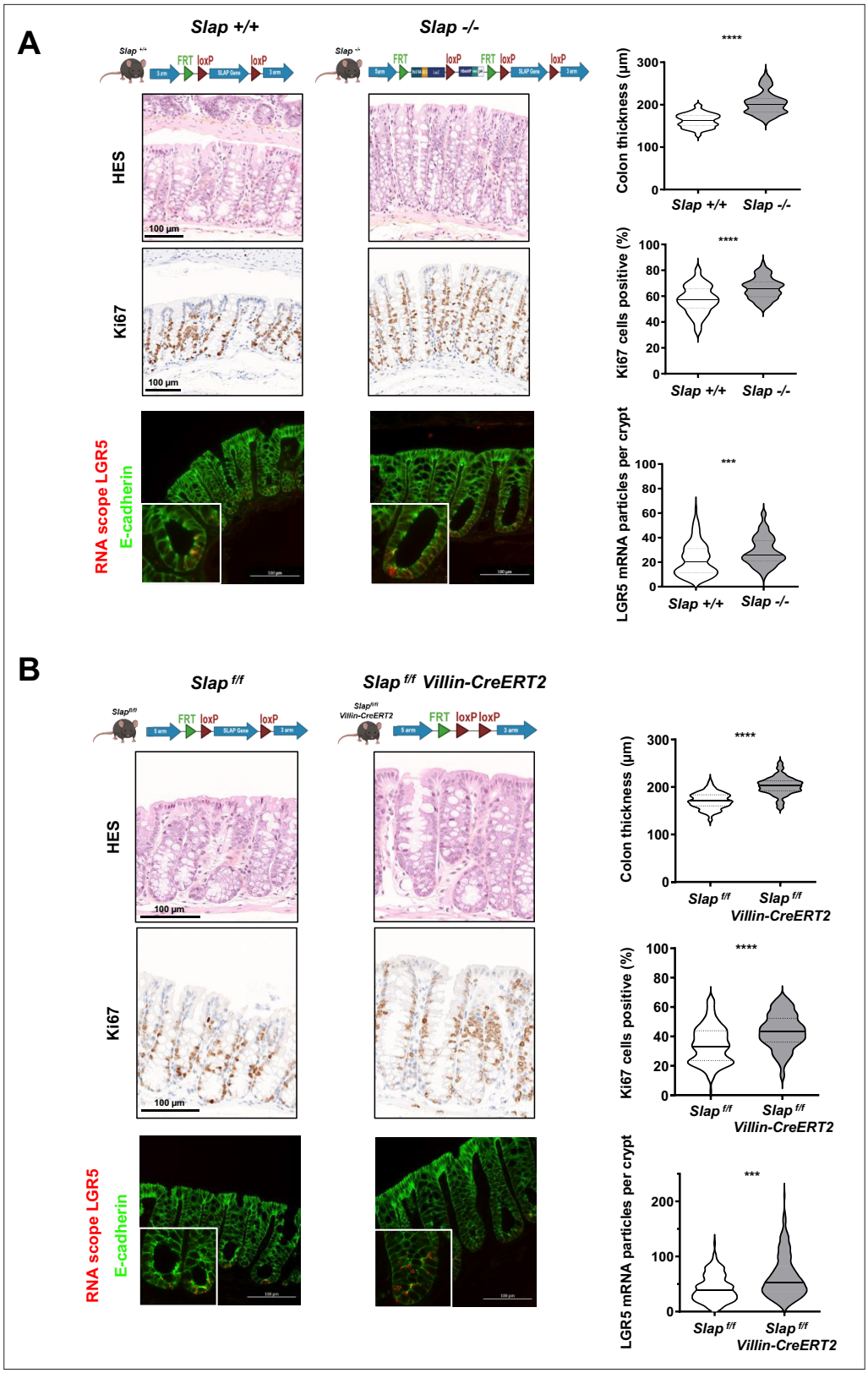


Figure 1. Murine Slap inactivation induces colonic epithelial hyperplasia. (**A**) Constitutive Slap deletion. Top: Hematoxylin and eosin (H&E) staining of transverse colon sections. Crypt thickness was measured and quantified as mean ± SEM from 25 to 40 crypts per mouse (n=6 female mice per group). Middle: Immunohistochemistry (IHC) for the proliferation marker Ki67, with quantification of Ki67-positive colonic epithelial cells (CECs). (mean

Figure 1 continued on next page

Figure 1 continued

± SEM from 20 to 40 crypts per mouse; n=5–6 mice per group). Bottom: RNAscope analysis of *Lgr5* to identify colonic stem cells, combined with E-cadherin immunofluorescence to delineate crypt architecture. Inset, higher (×4) magnification highlighting *Lgr5* expression. *Lgr5* RNA particles were quantified and are shown as mean ± SEM from 20 to 40 crypts per mouse (n=5–6 mice per group). ***p<0.001, ****p<0.0001 Mann–Whitney test. (**B**) Inducible epithelial-specific Slap deletion (villin-CreERT2). Top: H&E staining of transverse colon sections with quantification of crypt thickness (mean ± SEM from 25 to 40 crypts per mouse, n=6 mice/group). Middle: IHC for Ki67 with quantification of Ki67-positive CECs (mean ± SEM from 20 to 40 crypts per mouse; n=5–6 mice per group). Bottom: RNAscope analysis of Lgr5 combined with E-cadherin immunofluorescence; Inset, higher (×4) magnification highlighting *Lgr5* expression. Lgr5 RNA particles were quantified (mean ± SEM from 20 to 40 crypts per mouse, n=5–7 mice per group). Mice were analyzed at 3 months of age, 10 days after tamoxifen induction. ***p<0.001, ****p<0.0001 Mann–Whitney test.

The online version of this article includes the following figure supplement(s) for figure 1:

Figure supplement 1. Slap inactivation increases goblet cell numbers and SFK activity in the colon.

Cell-autonomous role of Slap in CEC proliferation

To determine if Slap functions in a cell-autonomous manner, we generated an inducible, intestinal-specific Slap-deficient mouse model by crossing *Slap flox/flox* mice with *villin-CreERT2* mice (*Slap* $^{f/f}$ *Villin CreERT2*). Tamoxifen (TAM) treatment for 10 days efficiently deleted Slap in the epithelium, as confirmed by a marked reduction in Slap immunofluorescence staining in the intestinal epithelium, while resident immune cells retained Slap expression (***Figure 1—figure supplement 1B***). Colonic Slap depletion recapitulated the phenotype of constitutive Slap-deficient mice, including increased colon thickness, enhanced CEC proliferation (***Figure 1B***), elevated goblet cell numbers (***Figure 1—figure supplement 1C***), and increased CSC activity (***Figure 1B***). To further investigate the cell-autonomous role of Slap in regulating CEC proliferation, we performed ex vivo analyses using isolated colonic crypts. Organoids derived from Slap-deficient epithelium were more numerous and larger than those from controls (***Figure 2A***).

Consistent with a role for Slap in restraining SFK signaling, Slap-deficient colonic crypts exhibited a two- to threefold increase in SFK activity and global cellular protein tyrosine phosphorylation (pTyr) levels (***Figure 2B***). An increase in protein tyrosine phosphorylation was also observed in organoids derived from Slap-deficient CECs and was reduced following treatment with the selective SFK inhibitor eCF506 (SRCi) (***Fraser et al., 2016***). Consistently, SRCi treatment decreased pSRC levels, confirming effective SFK inhibition (***Figure 2—figure supplement 1***). Functionally, the enhanced growth of Slap-deficient organoids was abolished by eCF506 treatment, demonstrating that the proliferative phenotype was SFK-dependent (***Figure 2C***). Together, these findings establish SLAP as a cell-autonomous suppressor of SFK-driven CEC proliferation.

Inducible Slap inactivation in the colon promotes colon tumorigenesis

We next evaluated Slap's role in colon tumorigenesis using the azoxymethane/dextran sulfate sodium (AOM/DSS) model of colitis-associated cancer, in which a single injection of the carcinogen AOM is followed by repeated cycles of DSS-induced colonic inflammation, leading to the development of colorectal tumors that recapitulate key features of inflammation-driven CRC (***Fazio et al., 2011***; ***Figure 3A***). In the inducible Slap knockout model, Slap deletion was initiated by TAM administration 10 days before AOM treatment and maintained by a second TAM administration at day 45 to ensure sustained Slap inactivation throughout tumor development (***Nguyen et al., 2025***). Under these conditions, Slap-deficient mice developed significantly more tumors and exhibited increased SFK activity within tumors compared with control animals (***Figure 3B***). Furthermore, tumoroids generated from these mice also showed enhanced growth, which was abolished by SFK kinase inhibition (***Figure 3C***), further supporting an SFK-dependent oncogenic mechanism. Interestingly, pharmacological SFK inhibition had no effect on tumoroids derived from control AOM/DSS-treated mice, consistent with previous reports that AOM/DSS-induced carcinogenesis involves oncogenic RAS mutations (***Takahashi and Wakabayashi, 2004***) and chronic inflammation. These findings suggest that while RAS-driven transformation can occur independently of SFK activity, Slap loss unleashes a parallel, SFK-dependent oncogenic pathway. The human relevance of this SLAP anti-oncogenic function was confirmed by modulating SLAP expression in CRC cells. In human SLAP-low HT29 and SW620

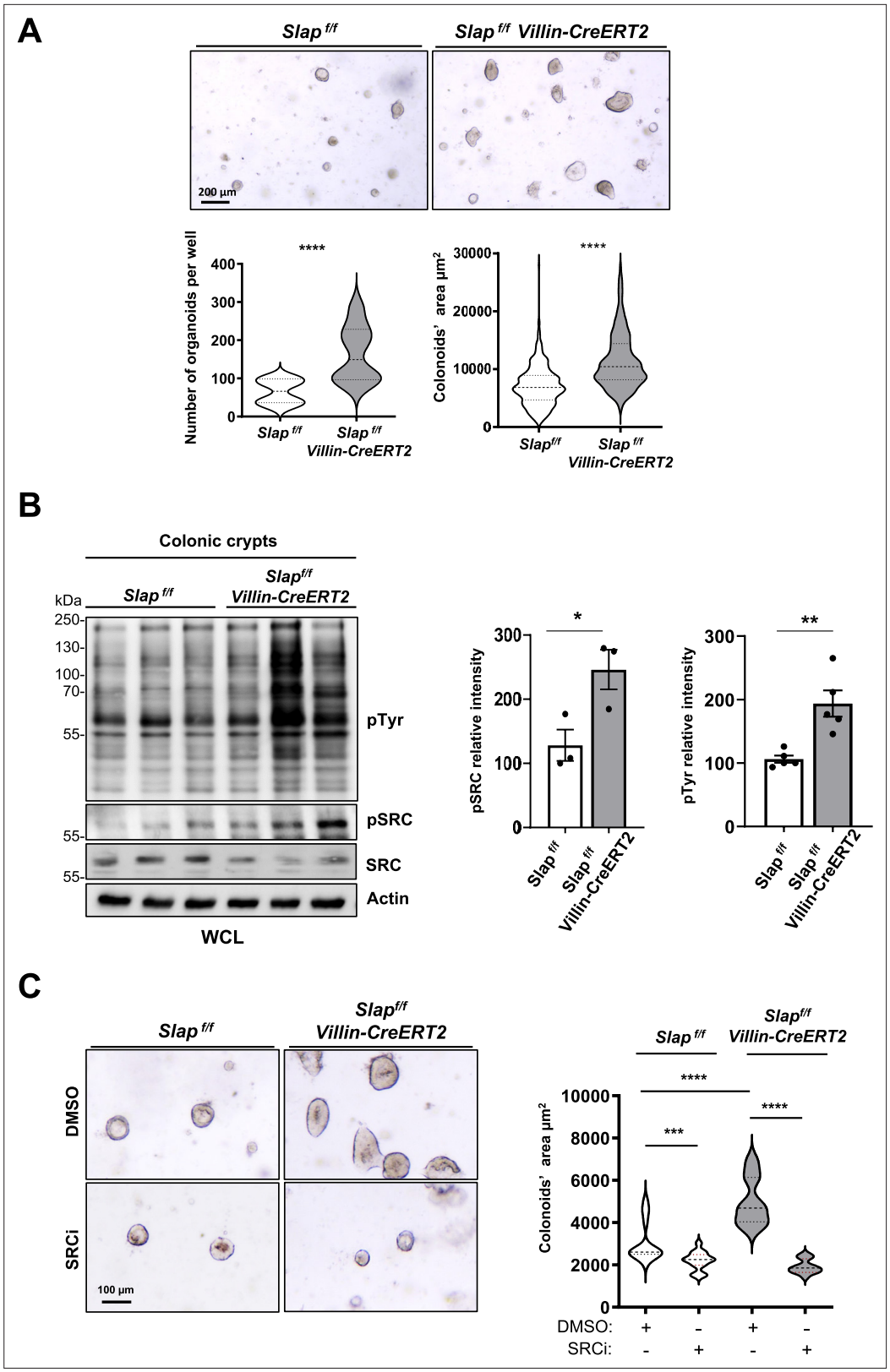


Figure 2. Intestinal Slap inactivation enhances colonic organoid development through SFK activation. (**A**) Slap-dependent colonic organoid development. Representative images of colon-derived organoids from *Slap* $^{f/f}$ and *Slap* $^{f/f}$ *Villin-CreERT2* mice cultured in Matrigel for 2 days. Quantification of organoid number and area is shown as mean ± SEM from 100 to 200 organoids per mouse (n=8 mice per group). ****p<0.0001 Mann–Whitney

Figure 2 continued on next page

Figure 2 continued

test. (**B**) Intestinal Slap deletion increases SFK activity and global protein tyrosine phosphorylation in colonic crypts. Representative immunoblots (right) and quantification (left) of phospho-SFK (pSRC) and total phosphotyrosine levels in lysates from isolated colonic crypts of the indicated genotypes. Data are presented as mean ± SEM from n=4–5 mice per group. *p<0.05; **p<0.001 t test. (**C**) Slap-dependent colonic organoid expansion requires SFK activity. Representative images and quantification of colon-derived organoids from *Slap* $^{f/f}$ and *Slap* $^{f/f}$ *Villin-CreERT2* mice cultured for 2 days in the presence or absence of the SRC-family kinase inhibitor eCF506 (100 nM). Data are shown as mean ± SEM from 100 to 200 organoids per mouse, n=4 mice per group. ***p<0.001, ****p<0.0001 Mann–Whitney test.

The online version of this article includes the following source data and figure supplement(s) for figure 2:

Source data 1. PDF file containing original western blots for ***Figure 2***, indicating the relevant bands.

Source data 2. Original files for western blot analysis displayed in ***Figure 2***.

Figure supplement 1. EPH-dependent phosphotyrosine accumulation and SFK activation in Slap-deficient colonic organoids.

Figure supplement 1—source data 1. PDF file containing original western blots for ***Figure 2–figure supplement 1***, indicating the relevant bands.

Figure supplement 1—source data 2. Original files for western blot analysis displayed in ***Figure 2–figure supplement 1***.

cell-lines, SLAP overexpression inhibited aldehyde dehydrogenase (ALDH) activity (***Figure 3—figure supplement 1A***), a well-established marker of CRC stem cells, as well as tumoroid growth (***Figure 3—figure supplement 1B***). Together, these results establish SLAP as a critical suppressor of SFK-driven colon tumorigenesis and cancer stem cell activity.

Slap target EphB2 to restrict SFK proliferative function in CEC

To investigate the Slap-dependent mechanism driving this phenotype, we hypothesized that Slap targets an upstream SFK activator within the RTK family that regulates colonic stem cells and CEC proliferation. Among RTKs expressed in colonic crypts, EphB2 and EphB3 are highly enriched in the CSC compartment and promote kinase-dependent CEC proliferation (***Batlle et al., 2002***; ***Genander et al., 2009***; ***Holmberg et al., 2006***). SFKs have also been reported as interactors and downstream effectors of EPHB2 signaling (***Chang et al., 2024***; ***Georgakopoulos et al., 2006***; ***Leroy et al., 2009***; ***Pasquale, 2024***; ***Zisch et al., 1998***). Supporting this model, western blotting analysis revealed elevated EphB2 protein levels in isolated Slap-deficient colonic crypts (***Figure 4A***), which was further confirmed by IHC analysis showing increased EphB2 expression throughout the colonic crypts of Slap-deficient mice (***Figure 4B***). This effect was recapitulated in CRC cells where enforced SLAP expression in SLAP-low HT29 cells decreased EPHB2 protein abundance. Interestingly, SLAP overexpression did not alter EPHB2 mRNA levels (***Figure 3—figure supplement 1A***), in accordance with a posttranslational mechanism involved in this process, as reported for EPHA2 (***Naudin et al., 2014***). Co-expression experiments in HEK293T cells revealed that EPHB2 associates with SLAP (***Figure 4C***), and this interaction required the SLAP SH2 and SH3 domains, as it was reduced with a SLAP mutant harboring inactive point mutations in the SH2 and SH3 domains (SLAP-mut; ***Figure 4C***; ***Mevizou et al., 2026***). The interaction also depended on phosphorylation of the juxta-membrane Tyr596 and Tyr602, which mediates SRC-SH2 binding (***Zisch et al., 1998***), because mutation of these residues to phenylalanine (YF EPHB2) diminished SLAP-EPHB2 binding (***Figure 4C***). Endogenous EPHB2 similarly interacted with SLAP in SLAP-expressing HT29 cells, confirming this association in CRC cells (***Figure 4—figure supplement 1B***). Consistent with enhanced EphB2 signaling, isolated Slap-deficient colonic crypts displayed increased EphB2 tyrosine phosphorylation together with elevated levels of associated phosphorylated SFKs (***Figure 4A***). Collectively, these findings identify EPHB2 as a novel SLAP interactor and target, supporting a role for SLAP in the regulation of EPHB2/SFK signaling.

We next asked whether EphB2 contributes to the Slap-dependent regulation of colonic organoid growth by inhibition of EphB2 kinase activity with the selective inhibitor ALW-II-49–7 (EPHB2i; ***Choi et al., 2009***; ***Noberini et al., 2012***; ***Zhang et al., 2026***). While EPHB2i had no effect on the growth of wild-type organoids, it markedly suppressed the enhanced growth observed in Slap-deficient organoids (***Figure 4C***). Treatment with the pan-EPH kinase inhibitor ALW-II-41–27 (pan-EPHi; ***Amato et al., 2014***; ***Choi et al., 2009***; ***Ferrao Blanco et al., 2024***) produced a similar reduction (***Figure 4C***),

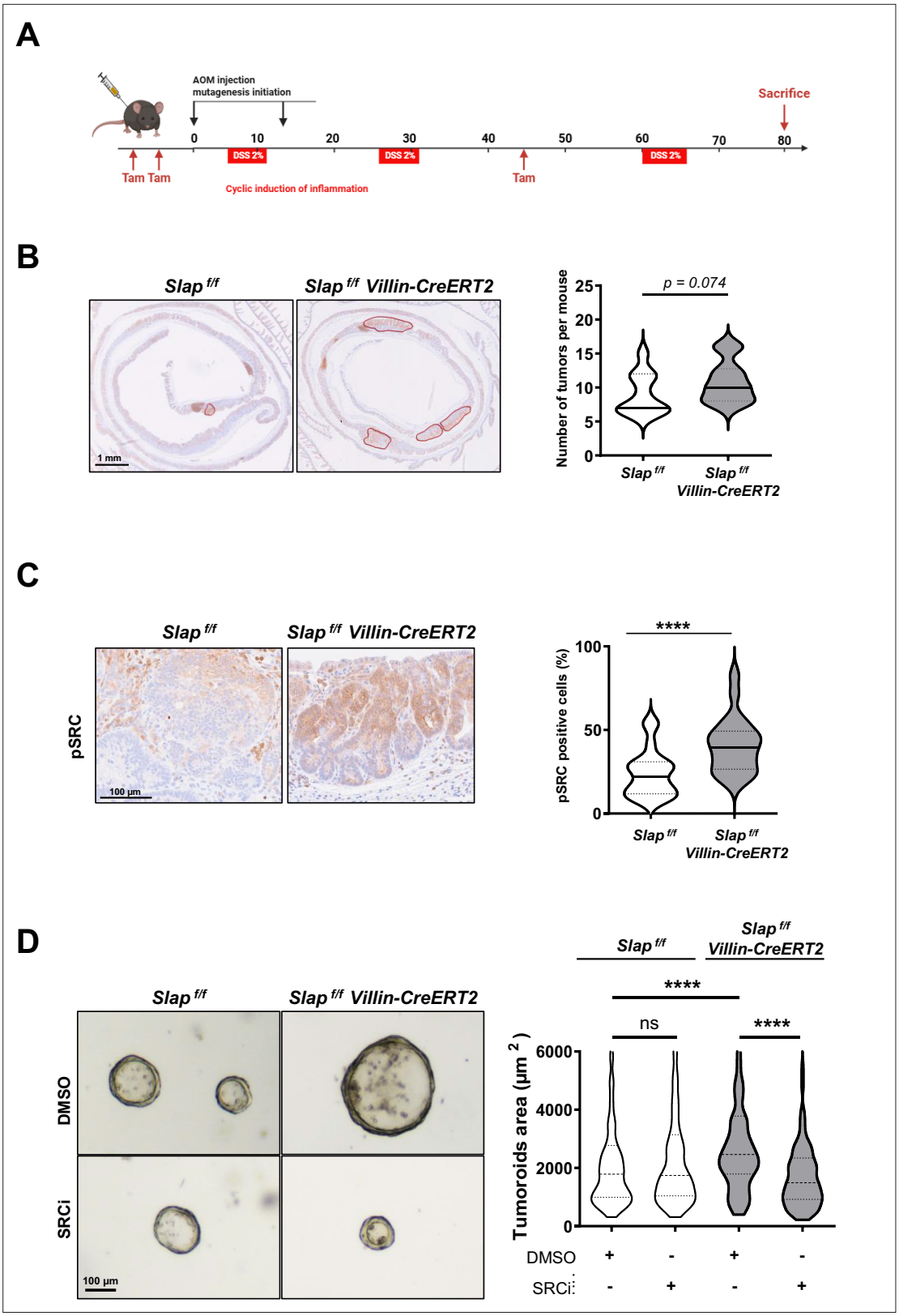


Figure 3. Inducible Slap intestinal inactivation drives colon tumorigenesis and promotes SFK-dependent tumoroid growth. (**A**) Experimental workflow of AOM/DSS-induced colon tumorigenesis. Mice received tamoxifen, followed 10 days later by a single azoxymethane (AOM) injection to induce mutagenesis and one cycle of dextran sodium sulfate (DSS) administered for 7 consecutive days. A second AOM injection was then performed, followed by two additional DSS cycles (7 days each). Mice were sacrificed at day 80. (**B**) Epithelial Slap loss accelerates colon tumor development.

Figure 3 continued on next page

Figure 3 continued

Left, representative H&E-stained sections showing transformed regions. Right, quantification of epithelial lesion area (mean ± SEM; n=11–15 mice per group). Statistical analysis is shown (Mann–Whitney test). (**C**) Slap depletion increases SFK activation in colonic tumors. Left, representative immunohistochemistry for phosphorylated SFK (pSRC) in transformed epithelium. Right, quantification of p-SFK–positive cells per mm² (mean ± SEM; n=7–9 mice per group; ****p<0.0001, Mann–Whitney test). (**D**) Tumoroids derived from *Slap* $^{f/f}$ and *Slap* $^{f/f}$ *Villin-CreERT2* mice were cultured in 3D Matrigel in the presence or absence of SRC inhibitor (SRCi) and imaged at day 3. Tumoroid area (μm²) was quantified following SRCi treatment (mean ± SEM; 150–250 organoids per mouse, n=4 mice per group; ns: p>0.05; ****p<0.0001, Mann–Whitney test).

The online version of this article includes the following figure supplement(s) for figure 3:

Figure supplement 1. SLAP suppresses human CRC stem cell properties.

supporting a role for EphB2 kinase activity in the Slap-dependent phenotype. Of note, EPHB2i did not alter the kinase activity of SRC expressed in HEK293T cells in contrast to EPHB2, arguing against a direct off-target effect on SFK (***Figure 3—figure supplement 1B***). Moreover, pEPHi reduced both the elevated phosphotyrosine levels and SFK activation induced by Slap deletion in colonic organoids (***Figure 2—figure supplement 1***), demonstrating that SFK hyperactivation in Slap-deficient CECs is dependent upon EphB2 signaling. Together, these data show that Slap limits colonic organoid growth by restricting EphB2-dependent activation of Src and reveal an EphB2-SFK signaling axis as a key driver of the hyperproliferative phenotype associated with Slap-deficiency (***Figure 4—figure supplement 1C***). Notably, a similar mechanism was observed in human CRC cells. Pharmacological inhibition of EPHB2 reduced tumoroid growth in a CRC model expressing low levels of SLAP, whereas this inhibitory effect was largely abolished upon SLAP overexpression. Importantly, a SLAP mutant (SLAP mut) that is unable to interact with EPHB2 fails to suppress tumoroid growth and restores sensitivity to EPHB2 inhibition, indicating that the tumor-suppressive activity of SLAP depends on its interaction with EPHB2 (***Figure 5A–C***). Collectively, these findings indicate that SLAP restrains the tumor-promoting activity of EPHB2 and suggest that the SLAP–EPHB2–SRC signaling axis is conserved between normal CECs and CRC.

Finally, we sought additional evidence supporting SLAP-EPHB2 signaling in CRC patients. We observed a weak but significant inverse correlation between SLAP expression and the colorectal CSC-like activity score in TCGA tumors (***Figure 5—figure supplement 1A***). In addition, although expression of EPHB2, SLAP, or the SLAP-related gene SLA2 alone was not associated with disease-free relapse in microsatellite-stable (MSS) CRC patients (***Figure 5—figure supplement 1B***), co-expression of SLAP and SLAP2 with EPHB2 was associated with improved prognosis (***Figure 5D***). Notably, this association was specific to MSS tumors, which are characterized by low immune infiltration, and was not observed in microsatellite instability (MSI) CRC, which displays high immune infiltration (***Figure 5D***). Together, these findings suggest that SLAP expression in tumor cells may contribute to the regulation of EPHB2-dependent CSC signaling in CRC.

Discussion

SFKs are potent drivers of intestinal stem cell proliferation and CRC, yet how their activity is restrained in normal epithelium remains unclear. Here, we identify the adaptor protein SLAP as a key epithelial-intrinsic regulator of SFK signaling in the colon. Epithelial loss of Slap increases proliferation, expands the stem cell compartment, and elevates SFK activation. Complementary organoid studies demonstrate that this requirement is cell autonomous. Importantly, pharmacologic SFK inhibition fully rescues the hyperproliferative phenotype of Slap-deficient organoids and tumoroids, revealing a crypt-intrinsic proliferative program that is SFK-dependent and normally constrained by Slap.

Mechanistically, our findings identify EPHB2 as a critical upstream activator of SRC signaling that is negatively regulated by SLAP. EPHB2 is highly expressed in intestinal stem and progenitor cells, where it contributes to crypt homeostasis and colorectal tumorigenesis (***Batlle et al., 2005***; ***Genander et al., 2009***; ***Holmberg et al., 2006***). We show that genetic loss of Slap results in elevated EPHB2 expression, increased SRC activation, and enhanced epithelial proliferation, whereas pharmacological inhibition of EPHB2 suppresses SRC activation and completely reverses the growth advantage of Slap-deficient organoids. Furthermore, EPHB2 inhibition selectively impairs the growth of CRC tumoroids expressing low levels of SLAP, supporting the existence of a conserved SLAP-EPHB2-SRC signaling axis in both normal and transformed intestinal epithelium.

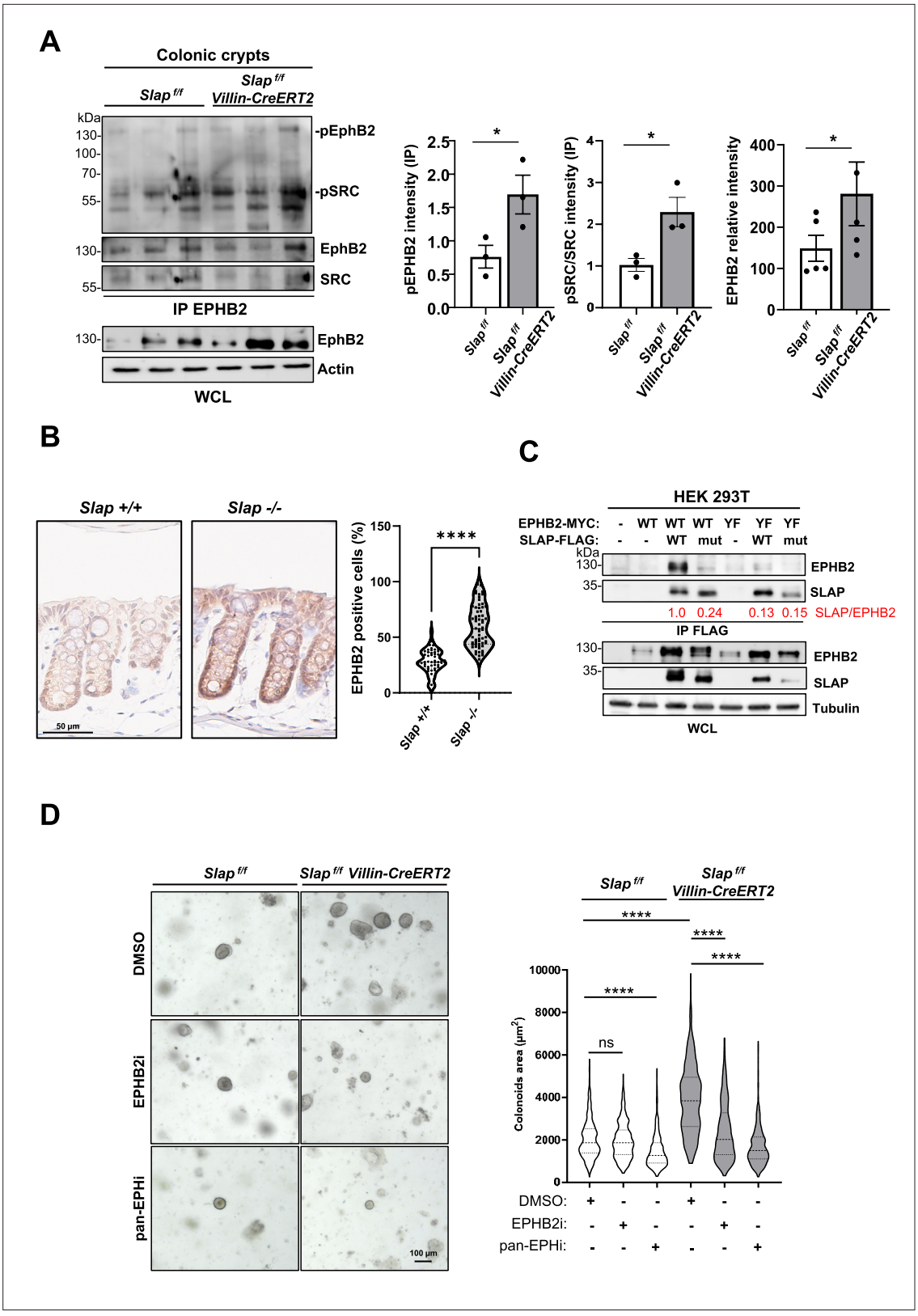


Figure 4. Slap targets EphB2 to restrict SFK proliferative signaling in CEC. (**A**) Intestinal Slap deletion increases EphB2 expression, EphB2 tyrosine phosphorylation, and its association with active SRC (pSRC) in colonic crypts. Left, quantification; right, representative immunoblots of EphB2 levels, EphB2 tyrosine phosphorylation, and associated pSRC following EphB2 immunoprecipitation from isolated colonic crypt lysates of the indicated mouse strains. Mean ± SEM; n=3–5 mice per group; *p<0.05, Student's t-test. (**B**) IHC analysis of EphB2 expression in colonic crypts from control and

Figure 4 continued on next page

Figure 4 continued

Slap-deficient mice. Left, representative images; right, quantification (mean ± SEM; n=3 mice per group; ****p<0.0001, Mann–Whitney test). (**C**) SLAP–EPHB2 interaction in HEK293T cells. Co-immunoprecipitation of the indicated SLAP-FLAG constructs (wild-type, WT; or SH3*SH2* mutant, SLAP mut) and EPHB2-MYC constructs (wild-type, WT; or Y596F/Y602F mutant, YF) transfected into HEK293T cells. Expression levels of SLAP and EPHB2 and relative quantification of SLAP-EPHB2 interaction are shown (representative example of three independent experiments). (**C**) Slap-dependent colon organoid expansion requires EphB2 activity. Representative images and quantification of colon-derived organoids from *Slap* $^{f/f}$ and *Slap* $^{f/f}$ *Villin-CreERT2* mice treated with the indicated EPH inhibitors (EPHB2i: 200 nM, pan-EPH2i: 100 nM, or DMSO control) and analyzed at day 2 (mean ± SEM; 150–200 organoids per mouse; n=4 mice per group; ns: p>0.05; ****p<0.0001, Mann–Whitney test).

The online version of this article includes the following source data and figure supplement(s) for figure 4:

Source data 1. PDF file containing original western blots for ***Figure 4***, indicating the relevant bands.

Source data 2. Original files for western blot analysis displayed in ***Figure 4***.

Figure supplement 1. SLAP interacts with EPHB2 and reduces its levels in HT29 cells.

Figure supplement 1—source data 1. PDF file containing original western blots for ***Figure 4—figure supplement 1***, indicating the relevant bands.

Figure supplement 1—source data 2. Original files for western blot analysis displayed in ***Figure 4—figure supplement 1***.

Although the precise molecular mechanism remains to be established, SLAP may restrain EPHB2 signaling through several non-mutually exclusive mechanisms. SLAP has been shown to promote the ubiquitin-dependent downregulation of multiple RTKs through interactions with E3 ubiquitin ligases, including CBL family proteins, UBE4A, and UBE3C (***Mevizou et al., 2026***; ***Myers et al., 2006***; ***Naudin et al., 2014***; ***Sirvent et al., 2008***; ***Zutshi et al., 2024***). Alternatively, SLAP may limit productive SRC recruitment and activation downstream of EPHB2 through its SH2 and SH3 domains (***Roche et al., 1998***). Future studies will be required to determine how SLAP controls EPHB2 abundance and signaling output in intestinal stem cells. In addition, other RTKs known to activate SFKs, including members of the EGFR family (***Cordero et al., 2014***; ***Wong et al., 2012***), may also contribute to the phenotype associated with SLAP loss. Moreover, Slap loss may affect EphB2's role in cell positioning (***Genander et al., 2009***; ***Holmberg et al., 2006***), contributing further to excessive proliferation.

Together, these findings establish SLAP as an epithelial tumor suppressor that limits SFK-driven stem cell proliferation and reveal a non-genetic mechanism of SRC oncogenic activation in CRC involving RTK hyperactivation (***Leroy et al., 2009***). More broadly, they suggest that SLAP loss may define CRC subsets with heightened dependence on SFK signaling, offering opportunities for therapeutic stratification and refinement of SRC-targeted interventions.

Materials and methods

Key resources table

Reagent type (species) or resource	Designation	Source or reference	Identifiers	Additional information
Strain, strain background (*Mus musculus*)	*Slap* ^{tm1a} mice	KOMP Repository	*Slap*^{tm1a} (KOMP); RRID:MMRRC_075158-UCD	C57BL/6 N background; LacZ reporter; FRT- and loxP-modified allele
Strain, strain background (*Mus musculus*)	*Slap -/-* mice	This study		Functional gene inactivation by LacZ cassette insertion
Strain, strain background (*Mus musculus*)	*Slap* $^{f/fl}$ mice	This study		Generated after FlpO-mediated recombination
Strain, strain background (*Mus musculus*)	Tg(CAG-flpo)1Afst	Kranz A et al., 2010	MGI:4453967; RRID:MMRRC_036512-UCD	Flp deleter mouse in C57Bl/6 based on Flpo recombinase
Strain, strain background (*Mus musculus*)	Tg(Vil1-cre/ERT2)23Syr	***el Marjou et al., 2004***	MGI:3053826; RRID:MGI:3053826	Tamoxifen-inducible Cre expression in intestinal epithelial cells
Strain, strain background (*Mus musculus*)	*Slap* $^{f/f}$ *Villin CreERT2* mice	This study		Conditional epithelial *SLA* knockout induced by tamoxifen
Cell line (human)	HT29	ATCC	HTB-38; RRID:CVCL_0320	Human colorectal adenocarcinoma
Cell line (human)	SW620	ATCC	CCL-227; RRID:CVCL_0547	Human colorectal adenocarcinoma

Continued on next page

Continued

Reagent type (species) or resource	Designation	Source or reference	Identifiers	Additional information
Cell line (human)	HEK293T	ATCC	CRL-3216, RRID:CVCL_0063	Human embryonic kidney cells used for transient transfection
Transfected construct (*M. musculus*)	SLAP-FLAG (WT)	***Naudin et al., 2014***		FLAG-tagged wild-type SLAP expression plasmid
Transfected construct (*M. musculus*)	SLAP-FLAG (SH3/SH2 mutant)	***Naudin et al., 2014***		FLAG-tagged SH3/SH2-deficient SLAP mutant expression plasmid
Transfected construct (human)	EPHB2-myc	***Narayanan et al., 2023***		Myc-tagged human EPHB2 expression plasmid
Transfected construct (human)	EPHB2 Y596F/Y602F mutant	This study		Myc-tagged human EPHB2 YF mutant expression plasmid
Sequence-based reagent	Mm-LGR5-C2	Bio-Techne	Catalog # 312178	RNAscope probe for detection of mouse LGR5
Antibody	Anti-Myc (mouse monoclonal)	Cell Signaling Technology	sc-2276S; RRID:AB_331783	WB (1:1000), IP (1:250)
Antibody	Anti-EPHB2 (rabbit monoclonal)	Cell Signaling Technology	sc-83029	WB (1:1000), IP (1:50)
Antibody	Anti-EPHB2 (goat polyclonal)	R&D Systems	Cat#AF467; RRID:AB_355375	IHC (1:100)
Antibody	Anti-FLAG M2 (mouse monoclonal)	Sigma-Aldrich	Clone M2; RRID:AB_262044	WB (1:1000), IP (1:250)
Antibody	Anti-HA (mouse monoclonal)	Invitrogen	Cat#26183; RRID:AB_10978021	WB (1:1000)
Antibody	Anti-β-actin (mouse monoclonal)	Sigma-Aldrich	Cat#A2228; RRID:AB_476697	WB (1:2000), (loading control)
Antibody	Anti-phosphotyrosine (4G10) (mouse monoclonal)	Gift from P. Mangeat	Clone 4G10; RRID:AB_2891016	WB (1:1000)
Antibody	Anti-SLAP (goat polyclonal)	Santa Cruz Biotechnology	sc-1215	WB (1:1000)
Antibody	Anti-phospho-SRC (rabbit polyclonal)	Invitrogen	PA5-97366; RRID:AB_2809160	WB (1:1000)
Antibody	Anti-phospho-SRC (rabbit polyclonal)	Cell Signaling Technology	Cat#2101; RRID:AB_331697	IHC (1:100)
Antibody	Alexa Fluor 488-conjugated secondary antibody (donkey polyclonal)	Jackson ImmunoResearch	Cat#711-545-152; RRID:AB_2340621	Fluorescence IHC (1:500)
Antibody	Cy3-conjugated secondary antibody (donkey polyclonal)	Jackson ImmunoResearch	Cat#711-165-152; RRID:AB_2307443	Fluorescence IHC (1:500)
Peptide, recombinant protein	Recombinant human R-spondin-1	PeproTech	Cat#78213	Organoid culture supplement
Peptide, recombinant protein	Recombinant human EGF	Bio-Techne	236-EG-200	Organoid culture supplement
Peptide, recombinant protein	Recombinant mouse Noggin	StemCell Technologies	Cat#78061	Organoid culture supplement
Peptide, recombinant protein	Recombinant mouse WNT3A	Thermo Fisher Scientific	Cat#315–20	Organoid culture supplement
Commercial assay or kit	ALDEFLUOR Kit	StemCell Technologies	Cat#01700	ALDH activity assay
Commercial assay or kit	RNeasy Plus Mini Kit	Qiagen	Cat#74134	RNA extraction
Commercial assay or kit	SuperScript VILO cDNA Synthesis Kit	Thermo Fisher Scientific	Cat#11754050	Reverse transcription
Commercial assay or kit	RNAscope Multiplex Fluorescent Reagent Kit	Bio-Techne	Cat#323100	RNA in situ hybridization assay for FFPE tissues
Commercial assay or kit	QuickChange Site-Directed Mutagenesis Kit	Agilent	Cat#200519	Site-directed mutagenesis
Commercial assay or kit	Tumor Dissociation Kit, Mouse	Miltenyi Biotec	Cat#130-096-730	Tumor dissociation
Commercial assay or kit	BIOXALL	Vector Laboratories	SP-6000–100	Endogenous Peroxidase and Alkaline Phosphatase Blocking Solution
Commercial assay or kit	DAB	Vector Laboratories	SK-4100	Chromogenic detection of HRP activity

Continued on next page

Continued

Reagent type (species) or resource	Designation	Source or reference	Identifiers	Additional information
Chemical compound, drug	Tamoxifen	Merck	Cat#5648–1 G	CreERT2 activation
Chemical compound, drug	Azoxymethane (AOM)	Sigma-Aldrich	Cat#A5486	Colon carcinogenesis model induction
Chemical compound, drug	Dextran sodium sulfate (DSS)	TdB Labs AB	DB001	Colitis induction
Chemical compound, drug	X-gal	Sigma-Aldrich	Cat#71077–3	β-Galactosidase staining
Chemical compound, drug	eCF506	MedChemExpress	Cat#HY-112096	SRC inhibitor
Chemical compound, drug	ALW-II-49–7	MedChemExpress	Cat#HY-18833	EPHB2 inhibitor
Chemical compound, drug	ALW-II-41–27	MedChemExpress	Cat#HY-18007	Pan-Eph inhibitor
Chemical compound, drug	Y-27632 dihydrochloride	Sigma-Aldrich	Cat#Y0503	Rock inhibitor
Chemical compound, drug	CHIR-99021	Tebu-Bio	Cat#10–1279	GSK3 inhibitor
Chemical compound, drug	N-acetyl-L-cysteine	Sigma-Aldrich	Cat#A9165	Organoid culture supplement
Other	Matrigel GFR phenol-red free	Corning	REF 356231	Basement Membrane Matrix for organoids and tumoroids
Other	Advanced DMEM/F12	Gibco	Cat#12634010	Basal culture medium
Other	B27 Supplement	Gibco	Cat#17504044	Serum-free supplement
Other	N2 Supplement	Gibco	Cat#17502048	Serum-free supplement
Other	GlutaMAX	Gibco	Cat#35050061	Cell culture supplement
Software, algorithm	GraphPad Prism	GraphPad Software	Version 9.3.1	Statistical analysis
Software, algorithm	ImageJ	NIH	RRID:SCR_003070	Image processing and quantification
Software, algorithm	NovoExpress	Agilent		Flow cytometry analysis
Software, algorithm	ZEN	Zeiss		Microscope image acquisition
Software, algorithm	NDP.view2	Hamamatsu	U12388-01	Image viewing
Software, algorithm	QuPath	***Bankhead et al., 2017***	RRID:SCR_018257	IHC quantification
Software, algorithm	GEPIA2	***Tang et al., 2019***	http://gepia2.cancer-pku.cn	TCGA gene expression and survival analyses

Generation of genetically modified mouse models

All mouse experiments were conducted in strict accordance with the European Community guidelines (86/609/EEC) and the French National Committee for the care and use of laboratory animals (87/848), complied with the ARRIVE guidelines, and were approved by the French Ministry of Higher Education, Research and Innovation (APAFIS#2022031511382008). All procedures were performed in the institutional animal facility (agreement #F3417216). Mice were housed in temperature-controlled ventilated cages (20–22 °C) under a 12 hr light/dark cycle, with relative humidity maintained between 45% and 55%, and were kept under pathogen-free conditions. *Slap*$^{tm1a(KOMP)}$ mice were generated from JM8A1.N3 embryonic stem cells (C57BL/6 N genetic background) produced by the trans-NIH KnockOut Mouse Project (KOMP) and obtained from the KOMP Repository (https://www.komp.org/). Genotyping was performed by PCR analysis of genomic DNA isolated from mouse tail biopsies. The *Slap*$^{tm1a(KOMP)}$, Tg(CAG-flpo)1Afst, and Tg(Vil1-cre/ERT2)23Syr mouse lines, as well as compound lines, were maintained on a C57BL/6 background and bred in a specific opportunistic pathogen-free (SOPF) facility, and experiments were conducted in a specific pathogen-free (SPF) facility.

Slap-inactivated mice (*Slap* -/-) were generated by insertion of a *LacZ* reporter cassette into the Slap locus, resulting in functional gene inactivation. The *LacZ* cassette was flanked by FRT sites, allowing recombination upon crossing with FlpO deleter mice. FlpO-mediated recombination generated the recombined *Slap* allele, whereas FlpO-negative littermates retaining the unrecombined *LacZ* allele were used as controls.

Inducible *Slap* knockout mice were generated by crossing Slap floxed mice with CreERT2 transgenic mice. TAM treatment induced Cre-mediated excision of the floxed Slap allele, resulting in gene

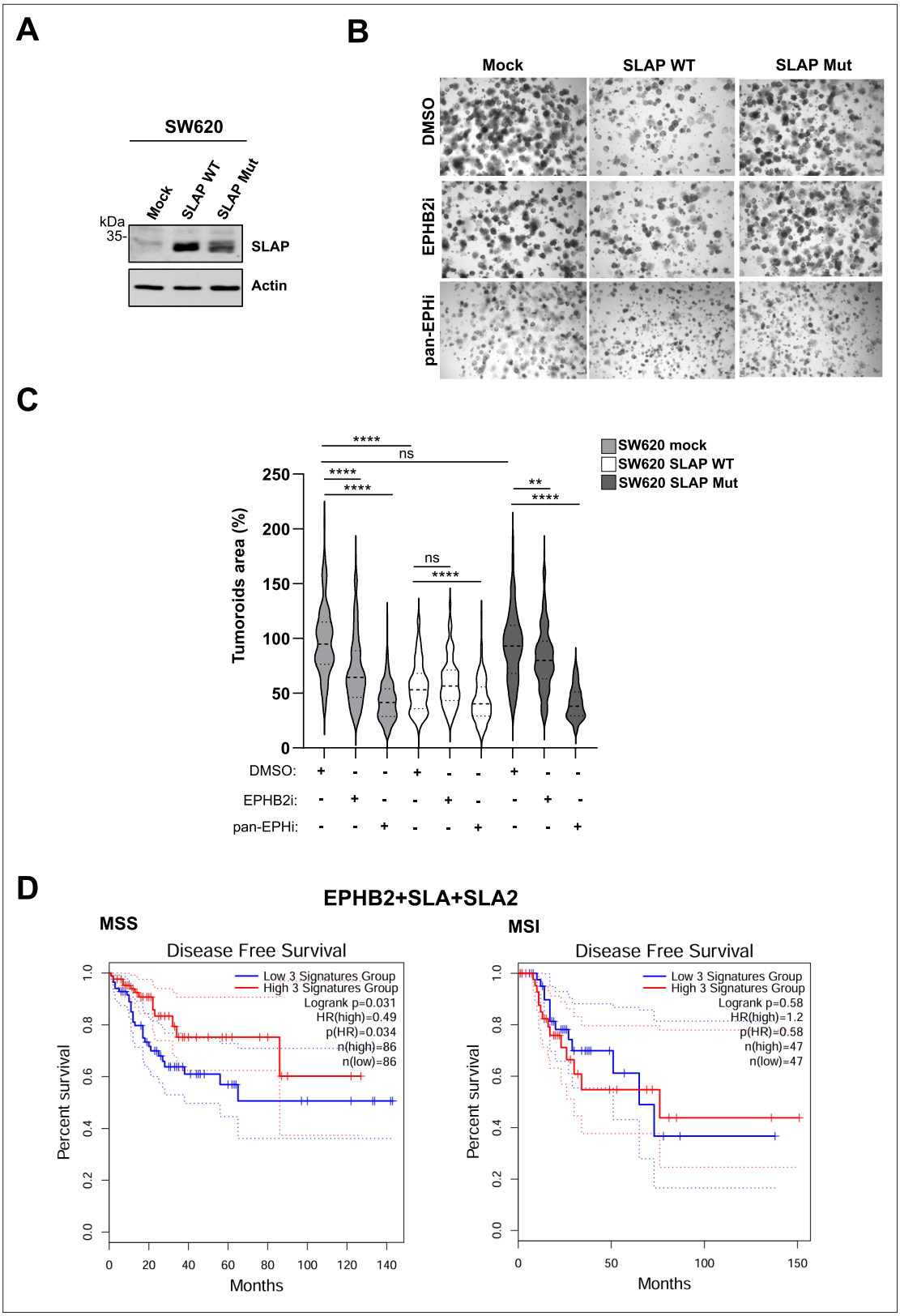


Figure 5. SLAP suppresses EPHB2-dependent tumoroid development of CRC cells and is associated with improved prognosis in MSS CRC. (**A**) SLAP expression in SW620 CRC cells transduced with empty vector (mock), wild-type SLAP, or an EPHB2-binding-defective SLAP mutant (SLAP Mut). (**B**) Representative tumoroid images from SW620 cells expressing mock, SLAP, or SLAP m and treated with indicated EPHB2 inhibitors (EPHB2i: 200 nM, pan-EPH2i: 100 nM, or DMSO control). (**C**) Quantification of tumoroid size from (**B**) (mean ± SEM; 150–200 tumoroids; n=3; ns: p>0.05; **p<0.001;

Figure 5 continued on next page

Figure 5 continued

***p<0.0005; ****p<0.0001, Mann–Whitney test). (**D**) Disease-free relapse analysis of TCGA MSS and MSI CRC patients stratified according to combined EPHB2, SLAP, and SLA2 expression. High SLAP/SLA2 and EPHB2 co-expression is associated with improved prognosis in MSS patients.

The online version of this article includes the following source data and figure supplement(s) for figure 5:

Source data 1. PDF file containing original western blots for ***Figure 5***, indicating the relevant bands.

Source data 2. Original files for western blot analysis displayed in ***Figure 5***.

Figure supplement 1. Contribution of SLAP expression to the regulation of EPHB2-dependent CSC signaling in CRC patients.

inactivation. To activate CreERT2, control and experimental mice received two intraperitoneal injections of TAM (2 mg per injection).

Mice genotyping

Mice tail biopsies underwent alkaline lysis and incubation at 92 °C for 20 min, followed by reaction neutralization. PCR amplification was conducted with the ready mix MyTAQRed mix (meridian). Resulting products were run on a 2% ethidium-bromide agarose gel (Sigma–Aldrich), using a 1 kb DNA ladder (Thermo Fisher Scientific), and imaged with a ChemiDoc MP system (Bio-Rad). The following primers were used: CSD-lacF: GCTACCATTACCAGTTGGTCTGGTGTC; CSD-neoF: GGGATCTCATGC TGGAGTTCTTCG; CSD-loxF: GAGATGGCGCAACGCAATTAATG; CSD-Sla-R: TCTCTGAGATGC CCCATTTTACCCC; CSD-Sla-ttR: GTTTCTTGGCACTGACTAGAGCAGG; CSD-Sla-F: GTTAACAA CACACCTACCCCTTGGC.

Chemical induction of tumorigenesis by AOM/DSS

Inducible epithelial SLAP knockout mouse model was treated with TAM to induce Slap depletion. DSS and AOM/DSS treatment was performed essentially as described in ***Nguyen et al., 2025***; ***Paul et al., 2022***. Briefly, 10 days following TAM treatment, a first AOM injection was performed. Shortly after the first round of DSS at 2% was given to the mice for 7 consecutive days. A week later another AOM injection was performed followed by two other rounds of DSS treatments two weeks apart. The mice were then sacrificed at day 80. Colons or tumors were then excised for tumoroids formation, cryopreservation or fixation followed with IHC analysis.

β-Galactosidase activity

To visualize the activity of the Slap promoter driving lacZ expression, we used 5-bromo-4-chloro-3-indolyl-beta-D-galactopyranoside (X-gal, Sigma-Aldrich) as described in ***Nguyen et al., 2025***. Organs were cryopreserved and 10 µm tissue sections were prepared. Sections were treated with 0.5% glutaraldehyde for 10 min at room temperature (RT) followed by overnight incubation at 37 °C in a staining solution containing 1 mg/ml X-gal, 5 mM potassium ferricyanide (K3Fe(CN)6), 5 mM potassium ferrocyanide (K4Fe(CN)6), and 2 mM MgCl2, 0.1% Triton in PBS-1X. The synthetic substrate X-gal gives an insoluble blue precipitate when cleaved by β-galactosidase. Samples were washed in PBS-1X for 5 min and rinsed briefly with dH2O before mounting with aqueous mounting medium (Sigma-Aldrich).

Immunohistochemistry of paraffin-embedded tissues

Fluorescent and bright-field immunohistochemistry on paraffin-embedded tissue. Intestinal tissues were fixed in neutral-buffered formalin for 24 hr at RT, embedded in paraffin, and tissue sections (4 µm) were prepared with a microtome (MICROM). Sections were incubated in successive baths of xylene and ethanol, and antigen retrieval was performed by boiling the sections with 10 mM sodium citrate (pH 6.4) or Tris-EDTA buffer (pH 9) for 20 min. Tissues were treated with TBS-1X2% serum, 0.1% Triton to block non-specific binding. Samples were then incubated with primary antibodies overnight at 4 °C. In the case of bright-field immunohistochemistry, sections were treated with BIOXALL (Vector Laboratories) for 10 min before blocking and incubation with primary antibodies. Secondary reagent staining was revealed using DAB (Vector Laboratories), and sections were counterstained with hematoxylin (Sigma-Aldrich) and then mounted with aqueous mounting medium (Sigma-Aldrich). As for fluorescence immunohistochemistry, sections were incubated in the presence of secondary antibodies conjugated to Alexa-488 or cyanin3 (Jackson ImmunoResearch Laboratories) and Hoechst

(2 µg/ml, Sigma–Aldrich) and mounted with aqueous mounting medium (Sigma-Aldrich). For histological analysis, the tissue sections were deparaffinized and stained with hematoxylin, eosin, and Alcian blue.

RNA in situ hybridization

ISH for Lgr5 was performed with the RNAscope FFPE assay kit (Bio-techne) according to the manufacturer's instructions. Briefly, 4 µm formalin-fixed, paraffin-embedded tissue sections were pretreated with heat and protease digestion and then hybridized with a target probe for Lgr5 (Probe - Mm-LGR5-C2, Biotechne). Thereafter, a fluorophore signal amplification system was hybridized to the target probe.

RNA extraction and qPCR

Total RNA was extracted using RNeasy Plus Mini Kit columns (Qiagen). First-strand cDNA synthesis was performed with 1 µg of purified RNA using SuperScript VILO cDNA synthesis KIT (Thermo Fisher Scientific) according to the manufacturer's instructions. qRT-PCR experiments were performed using LightCycler 480 SYBR Green I Master (Roche Diagnostics) on the LightCycler 480 system using the following primers: EHPB2_F 5'-CGGCTGCATGTCCCTCATC-3', EHPB2_R 5'-GTCCCCGTTACAGTAG AGCTT-3'; GAPDH_F 5'-TCTCCTCTGACTTCAACAGCGAC-3' & GAPDH_R 5'-CCCTGTTGCTGT AGCCAAATTC-3'. Relative expression was determined using the threshold cycle relative quantification method. Data were normalized to the expression levels of GAPDH.

ALDH analysis

The ALDH assay was performed as described in ***Nguyen et al., 2025*** and according to the protocol of the ALDEFLUORTM kit (#01700, Stemcell). FACS analysis was performed through the Novocyte ACEA 2 fluorescence-activated cell sorting flow cytometer, and data were analyzed using NovoExpress software.

Antibodies and reagents

Antibodies used for biochemistry: anti-Myc (#2276 S, CST), anti-EphB2 D2X2 I (#83029, CST), anti-EphB2 (for IHC, # AF467 R&D Systems), anti-FLAG (M2 antibody, Sigma-Aldrich), anti-HA (Invitrogen, # 26183), anti-Actin (Sigma-Aldrich, #A2228), anti-pTyr 4G10 (gift from P. Mangeat, CRBM, Montpellier, France), and anti-SLAP clone C-19 (Santa Cruz Biotechnology, sc-1215). SFK activity was assessed using an anti-phospho-SRC antibody (Invitrogen, PA5-97366 for WB, and #2101 from CST for IHC), which also cross-reacts with other p-SFKs, revealed increased SFK activity. All antibodies utilized in IHC were used according to supplier protocols. SFK activities were revealed with the help of SignalStain Boost IHC Detection Reagent. Inhibitors used in this study: SRCi eCF506 (MedChemExpress, #HY-112096), EPHB2 inhibitor ALW-II-49–7 (EPHB2i, MedChemExpress, #HY-18833), Pan Eph inhibitor ALW-II-41–27 (pan-EPHi, MedChemExpress, # HY-18007). SLAP-FLAG (WT and SH3*SH2* mutant, mut) constructs were described in ***Naudin et al., 2014***. EPHB2-myc construct was from ***Narayanan et al., 2023***. EPHB2 Y596F/Y602F mutant (YF mutant) was obtained by QuickChange Site-Directed Mutagenesis Kit (Agilent) using the following oligonucleotides: 5′-gaccccaggcatgaagatctTcat cgatcctttcacctTcgaggaccccaacgaggcag-3′ and 5′-ctgcctcgttggggtcctcgAaggtgaaaggatcgatgAagatc ttcatgcctggggtc-3′. Other reagents: Advanced DMEM/F12 (Gibco), B27 supplement (Thermo Fisher Scientific), N2 supplement (Thermo Fisher Scientific), GlutaMAX (Thermo Fisher Scientific), Hepes (Thermo Fisher Scientific), N-acetyl cysteine (Sigma-Aldrich), CHIR-99021 (Tebu-BIO), Recombinant human R-spondin-1 (Peprotech). TAM (Merck group), Azoxymlethane (Sigma-Aldrich).

Cell culture and transfections

HT29, SW620, and HEK293T cell lines were directly obtained from ATCC (Rockville, MD), expanded from early-passage frozen stocks, and used for experiments within six months after thawing. HT29 and SW620 cells stably expressing SLAP (or mock as a control) were described in ***Mevizou et al., 2026***; ***Naudin et al., 2014***. Cells were cultured at 37 °C and 5% CO2 in a humidified incubator in Dulbecco's modified Eagle's medium (DMEM) GlutaMAX (Invitrogen) supplemented with 10% fetal calf serum (FCS), 100 U/ml of penicillin, and 100 µg/ml of streptomycin, and were routinely tested (once a week) for Mycoplasma using MycoAlert Mycoplasma detection kit (Lonza, #LT07-318). Transient

plasmid transfections in HEK293T cells were performed with the jetPEI reagent (Polyplus-transfection) according to the manufacturer's instructions.

Biochemistry

Co-immunoprecipitation and western blotting (WB) were described in ***Mevizou et al., 2026***; ***Naudin et al., 2014***. Cells or isolated colonic crypts were lysed on ice using lysis buffer (20 mM Hepes pH 7.5, 150 mM NaCl, 0.5% Triton X-100, 6 mM β-octylglucoside), supplemented with complete mini EDTA-free protease and phosphatase inhibitor cocktail tablets (Roche). Protein lysates (15–35 µg) were resolved by SDS-PAGE, transferred to LF/PVDF membranes using the Trans-Blot Turbo system (Bio-Rad), and incubated overnight at 4 °C with the appropriate primary antibody (1:1000). For immunoprecipitation (IP), antibodies were used at 1:100. Membranes were then incubated for 45 min with the HRP-conjugated secondary antibody (Cell Signaling, 1:4000). Signals were detected using ECL Plus (Amersham Biosciences) and imaged with the Amersham Imager 600 (GE Healthcare Life Sciences). Signal quantification and analysis were carried out using ImageJ software. For SLAP-EPHB2 association experiments, HEK293T cells were co-transfected for 48 hr with the indicated FLAG-tagged and EPHB2 constructs either WT or the YF EPHB2 mutant. Endogenous EPHB2 association experiments were performed in HT29 cells stably expressing SLAP-FLAG. Cell-lysates were subjected to SLAP-FLAG immunoprecipitation using anti-FLAG magnetic beads (#A3697, Pierce). EPHB2-myc was immunoprecipitated using MYC-Tag (9B11) mouse monoclonal antibody (#2276, CST) and protein G sepharose beads (Thermo Fisher Scientific).

Organoids derived from colonic crypts

Inducible epithelial Slap knockout models were sacrificed 10 days after TAM induction. Organoids were performed as described in ***Nguyen et al., 2025***. Briefly, the colons were collected and washed with PBS containing antibiotics. They were then cut open and further dissected into small pieces, then washed with a wash buffer containing PBS 1 x, penicillin, streptomycin (Gibco), and Fungin (Invivo Gen) until the supernatant is clear. These pieces were then incubated in a crypt isolation buffer on ice for 30 min (wash buffer, 1% BSA fraction, and 25 mM EDTA). Crypt fractions were then isolated after thorough pipetting, centrifuged at 300 × *g*, 4 °C for 5 min. 500 crypts were resuspended in M1 medium mixture Advanced DMEM/F12 supplemented with 1% Penstrep, 1% Fungin, 10 mM Hepes, 1% GlutaMAX, N-2, B-27, 1 Mm N-acetyl cysteine, and Matrigel (Corning; ratio 1:2). The mixture was plated in a 24-well plate. After Matrigel polymerization, 500 µl of M2 medium M1 media supplemented with EGF (50 ng/ml, Bio-techne), Noggin (100 ng/ml, Stem cell technologies), R-spondin1 (500 ng/ml, Stem cell technologies), Y27 (10 µM, Sigma-Aldrich), CHIR-99021 (3 µM, Tebu-Bio), and WNT3a (50 n/ml, Thermo Fisher Scientific) was added to each well containing or not the SRC inhibitor eCF506 (100 nM, Medchem express) and in other cases the EphB inhibitors EPHB2i (ALW-II-49–7, 200 nM) and the pan-EPH inhibitor pan-EPHi (ALW-II-41–27, 100 nM, Medchem express). For organoids derived from AOM/DSS transformed CECs, tumors were excised from mice treated with AOM/DSS at day 80. They were dissociated using the Tumor Dissociation Kit mouse (Miltenyi Biotec). The dissociation was then stopped by DMEM medium containing 10% SVF. The mixture was then centrifuged, and the pellet was resuspended in DMEM F12 without factors. Cells were counted and plated at almost 10,000 cells per well in a 24-well plate in a mixture containing 3D Matrigel. After 30 min of incubation, a complete F12 medium was added to the solidified domes containing or not the SRC inhibitor eCF506 (100 nM) (***Fraser et al., 2016***).

Tumoroids-derived from CRC cells

2000–5,000,000 human CRC cells were resuspended in Advanced DMEM/F12 supplemented with 1% Penstrep, 2 mM L-glutamine, N-2, and Matrigel (Corning) (1:2 ratio) prior to plating in 24-well plates. After polymerization of Matrigel, 0.5 ml Advanced DMEM/F12 supplemented with EGF (20 ng/ml, Biotechne) and FGF (10 ng/ml, Biotechne) was added. Tumoroids were cultured at 37 °C and 5% CO_2 in a humidified incubator.

Microscopy and imaging

Histological slides were digitized using a Nanozoomer scanner (Hamamatsu) with a ×40 objective and viewed with NDP.view2 software (Hamamatsu). Fluorescence images were captured using an

AxioImager Z2 microscope (Zeiss) operated with Zen software. Image processing was performed in ImageJ.

TCGA COAD analysis

Gene expression and clinical data from the TCGA colon adenocarcinoma (COAD) cohort were analyzed using GEPIA2 (http://gepia2.cancer-pku.cn/). Kaplan–Meier disease-free survival analyses were performed using the GEPIA2 Survival Analysis module, with patients stratified into high- and low-expression groups based on the median expression value. Stem cell-like signature scores were calculated using the GEPIA2 Signature Score module (***Merlos-Suárez et al., 2011***) from the indicated gene set, and associations with disease-free survival were assessed by log-rank testing.

Statistical analysis

All analysis was performed using GraphPad Prism (9.3.1). Data are presented as the mean ± SEM. The Mann-Whitney test was used. The statistical significance level is illustrated with p values: *p≤0.05, **p≤0.01, ***p≤0.001, **** p≤0.0001 (t-test).

Acknowledgements

We thank the PCEA, ZEFI, Centre d'Ingénierie Génétique Murine, and RHEM platforms animal facilities, immunohistochemistry analyses, Montpellier Rio Imaging (MRI) platform, Valérie PINET, Ethan ALBERT, Hahne's and PANNEQUIN's teams, and our colleagues for discussion and technical support. This work was supported by La Ligue Nationale Contre le Cancer (LNCC) through the Labelling Team programs 2017 and 2020, La Fondation pour la Recherche Médicale through the Labelling Team program 2023 and ARC charity. Additional support was provided by the Montpellier SIRIC grant "INCa-DGOS-Inserm 6045," CNRS, and the University of Montpellier. The MRI platform, a member of the national infrastructure France-BioImaging (https://ror.org/01y7vt929) is supported by the French National Research Agency (ANR-24-INBS-0005 FBI BIOGEN). The RHEM facility is supported by the SIRIC Montpellier Cancer grant INCa_Inserm_DGOS_12553, the European Regional Development Fund and the Occitanie region (FEDER-FSE 2014–2020 Languedoc-Roussillon), and La Ligue Contre le Cancer for processing animal tissues and histology. DN was supported by the Montpellier University and LNCC. SR is an INSERM investigator.

Additional information

Funding

Funder	Grant reference number	Author
Fondation pour la Recherche Médicale	FRM2023	Dana Naim Zouheir Houhou Florent Cauchois Kevin Espie Yvan Boublik Julie Nguyen Audrey Sirvent Serge Roche
La Ligue Contre le Cancer	LIGUE2020	Dana Naim Yvan Boublik Julie Nguyen
La Ligue Contre le Cancer	LIGUE2022	Conception Paul Michael Hahne

The funders had no role in study design, data collection and interpretation, or the decision to submit the work for publication.

Author contributions

Dana Naim, Resources, Data curation, Formal analysis, Investigation, Visualization, Methodology; Zouheir Houhou, Florent Cauchois, Kevin Espie, Zeinab Homayed, Conception Paul, Investigation,

Methodology; Valerie Simon, Yvan Boublik, Julie Pannequin, Resources, Methodology; Francina Langa Vives, Resources; Morgan Maillard, Resources, Formal analysis; Michael Hahne, Conceptualization, Resources; Julie Nguyen, Supervision, Investigation, Methodology; Audrey Sirvent, Conceptualization, Resources, Data curation, Formal analysis, Supervision, Validation, Investigation, Visualization, Methodology, Writing – review and editing; Serge Roche, Conceptualization, Formal analysis, Supervision, Funding acquisition, Validation, Investigation, Methodology, Writing – original draft, Project administration, Writing – review and editing

Author ORCIDs
Dana Naim https://orcid.org/0000-0002-4982-8381
Zouheir Houhou https://orcid.org/0009-0009-0535-0505
Morgan Maillard https://orcid.org/0000-0003-0062-2507
Julie Pannequin https://orcid.org/0000-0002-9956-373X
Julie Nguyen https://orcid.org/0000-0002-8361-0204
Audrey Sirvent https://orcid.org/0000-0003-4555-6312
Serge Roche https://orcid.org/0000-0003-3413-3859

Ethics
Mouse experiments were conducted in strict accordance with the European Community guidelines (86/609/EEC) and the French National Committee for the care and use of laboratory animals (87/848), complied with the ARRIVE guidelines, and were approved by the French Ministry of Higher Education, Research, and Innovation (APAFIS#2022031511382008).

Peer review material
Version of Record:
Reviewer #1 (Public review): https://doi.org/10.7554/eLife.110324.3.sa1
Reviewer #2 (Public review): https://doi.org/10.7554/eLife.110324.3.sa2
Author response https://doi.org/10.7554/eLife.110324.3.sa3

Reviewed preprint v2
Reviewer #1 (Public review): https://doi.org/10.7554/eLife.110324.2.sa2
Reviewer #2 (Public review): https://doi.org/10.7554/eLife.110324.2.sa1
Author response: https://doi.org/10.7554/eLife.110324.2.sa0
eLife Assessment https://doi.org/10.7554/eLife.110324.2.sa3

Reviewed preprint v1
Reviewer #1 (Public review): https://doi.org/10.7554/eLife.110324.1.sa2
Reviewer #2 (Public review): https://doi.org/10.7554/eLife.110324.1.sa1
Author Response: https://doi.org/10.7554/eLife.110324.1.sa0
eLife Assessment https://doi.org/10.7554/eLife.110324.1.sa3

Additional files

Supplementary files
MDAR checklist

Data availability
Data supporting the findings of this study are all included in the manuscript, figures, figure supplements, and source data files.

References

Amato KR, Wang S, Hastings AK, Youngblood VM, Santapuram PR, Chen H, Cates JM, Colvin DC, Ye F, Brantley-Sieders DM, Cook RS, Tan L, Gray NS, Chen J. 2014. Genetic and pharmacologic inhibition of EPHA2 promotes apoptosis in NSCLC. *The Journal of Clinical Investigation* **124**:2037–2049. DOI: https://doi.org/10.1172/JCI72522, PMID: 24713656

Bankhead P, Loughrey MB, Fernández JA, Dombrowski Y, McArt DG, Dunne PD, McQuaid S, Gray RT, Murray LJ, Coleman HG, James JA, Salto-Tellez M, Hamilton PW. 2017. QuPath: Open source software for

digital pathology image analysis. *Scientific Reports* **7**:16878. DOI: https://doi.org/10.1038/s41598-017-17204-5, PMID: 29203879

Barker N, van Es JH, Kuipers J, Kujala P, van den Born M, Cozijnsen M, Haegebarth A, Korving J, Begthel H, Peters PJ, Clevers H. 2007. Identification of stem cells in small intestine and colon by marker gene Lgr5. *Nature* **449**:1003–1007. DOI: https://doi.org/10.1038/nature06196

Batlle E, Henderson JT, Beghtel H, van den Born MMW, Sancho E, Huls G, Meeldijk J, Robertson J, van de Wetering M, Pawson T, Clevers H. 2002. Beta-catenin and TCF mediate cell positioning in the intestinal epithelium by controlling the expression of EphB/ephrinB. *Cell* **111**:251–263. DOI: https://doi.org/10.1016/s0092-8674(02)01015-2, PMID: 12408869

Batlle E, Bacani J, Begthel H, Jonkeer S, Gregorieff A, van de Born M, Malats N, Sancho E, Boon E, Pawson T, Gallinger S, Pals S, Clevers H. 2005. EphB receptor activity suppresses colorectal cancer progression. *Nature* **435**:1126–1130. DOI: https://doi.org/10.1038/nature03626

Chang C, Banerjee SL, Park SS, Zhang XL, Cotnoir-White D, Opperman KJ, Desbois M, Grill B, Kania A. 2024. Ubiquitin ligase and signalling hub MYCBP2 is required for efficient EPHB2 tyrosine kinase receptor function. *eLife* **12**:RP89176. DOI: https://doi.org/10.7554/eLife.89176, PMID: 38289221

Choi Y, Syeda F, Walker JR, Finerty PJ, Cuerrier D, Wojciechowski A, Liu Q, Dhe-Paganon S, Gray NS. 2009. Discovery and structural analysis of Eph receptor tyrosine kinase inhibitors. *Bioorganic & Medicinal Chemistry Letters* **19**:4467–4470. DOI: https://doi.org/10.1016/j.bmcl.2009.05.029

Cordero JB, Ridgway RA, Valeri N, Nixon C, Frame MC, Muller WJ, Vidal M, Sansom OJ. 2014. c-Src drives intestinal regeneration and transformation. *The EMBO Journal* **33**:1474–1491. DOI: https://doi.org/10.1002/embj.201387454, PMID: 24788409

Daud AI, Krishnamurthi SS, Saleh MN, Gitlitz BJ, Borad MJ, Gold PJ, Chiorean EG, Springett GM, Abbas R, Agarwal S, Bardy-Bouxin N, Hsyu PH, Leip E, Turnbull K, Zacharchuk C, Messersmith WA. 2012. Phase I study of bosutinib, a src/abl tyrosine kinase inhibitor, administered to patients with advanced solid tumors. *Clinical Cancer Research* **18**:1092–1100. DOI: https://doi.org/10.1158/1078-0432.CCR-11-2378, PMID: 22179664

Dragone LL, Myers MD, White C, Gadwal S, Sosinowski T, Gu H, Weiss A. 2006a. Src-like adaptor protein (SLAP) regulates B cell receptor levels in a c-Cbl-dependent manner. *PNAS* **103**:18202–18207. DOI: https://doi.org/10.1073/pnas.0608965103, PMID: 17110436

Dragone LL, Myers MD, White C, Sosinowski T, Weiss A. 2006b. SRC-like adaptor protein regulates B cell development and function. *The Journal of Immunology* **176**:335–345. DOI: https://doi.org/10.4049/jimmunol.176.1.335, PMID: 16365426

el Marjou F, Janssen K-P, Chang BH-J, Li M, Hindie V, Chan L, Louvard D, Chambon P, Metzger D, Robine S. 2004. Tissue-specific and inducible Cre-mediated recombination in the gut epithelium. *Genesis* **39**:186–193. DOI: https://doi.org/10.1002/gene.20042, PMID: 15282745

Fazio V, Robertis M, Massi E, Poeta M, Carotti S, Morini S, Cecchetelli L, Signori E. 2011. The AOM/DSS murine model for the study of colon carcinogenesis: From pathways to diagnosis and therapy studies. *Journal of Carcinogenesis* **10**:9. DOI: https://doi.org/10.4103/1477-3163.78279

Ferrao Blanco MN, Lesage R, Kops N, Fahy N, Bekedam FT, Chavli A, Bastiaansen-Jenniskens YM, Geris L, Chambers MG, Pitsillides AA, Narcisi R, van Osch GJVM. 2024. A multi-model approach identifies ALW-II-41-27 as a promising therapy for osteoarthritis-associated inflammation and endochondral ossification. *Heliyon* **10**:e40871. DOI: https://doi.org/10.1016/j.heliyon.2024.e40871, PMID: 39717596

Fraser C, Dawson JC, Dowling R, Houston DR, Weiss JT, Munro AF, Muir M, Harrington L, Webster SP, Frame MC, Brunton VG, Patton EE, Carragher NO, Unciti-Broceta A. 2016. Rapid discoveryand structure–activity relationshipsof pyrazolopyrimidines that potently suppress breast cancer cell growthvia SRC kinase inhibition with exceptional selectivity over ABL kinase. *Journal of Medicinal Chemistry* **59**:4697–4710. DOI: https://doi.org/10.1021/acs.jmedchem.6b00065

Genander M, Halford MM, Xu NJ, Eriksson M, Yu Z, Qiu Z, Martling A, Greicius G, Thakar S, Catchpole T, Chumley MJ, Zdunek S, Wang C, Holm T, Goff SP, Pettersson S, Pestell RG, Henkemeyer M, Frisén J. 2009. Dissociation of EphB2 signaling pathways mediating progenitor cell proliferation and tumor suppression. *Cell* **139**:679–692. DOI: https://doi.org/10.1016/j.cell.2009.08.048, PMID: 19914164

Georgakopoulos A, Litterst C, Ghersi E, Baki L, Xu C, Serban G, Robakis NK. 2006. Metalloproteinase/Presenilin1 processing of ephrinB regulates EphB-induced Src phosphorylation and signaling. *The EMBO Journal* **25**:1242–1252. DOI: https://doi.org/10.1038/sj.emboj.7601031, PMID: 16511561

Holmberg J, Genander M, Halford MM, Annerén C, Sondell M, Chumley MJ, Silvany RE, Henkemeyer M, Frisén J. 2006. EphB receptors coordinate migration and proliferation in the intestinal stem cell niche. *Cell* **125**:1151–1163. DOI: https://doi.org/10.1016/j.cell.2006.04.030, PMID: 16777604

Imada S, Murata Y, Kotani T, Hatano M, Sun C, Konno T, Park JH, Kitamura Y, Saito Y, Ohdan H, Matozaki T. 2016. Role of Src family kinases in regulation of intestinal epithelial homeostasis. *Molecular and Cellular Biology* **36**:2811–2823. DOI: https://doi.org/10.1128/MCB.00311-16, PMID: 27550814

Irby RB, Mao W, Coppola D, Kang J, Loubeau JM, Trudeau W, Karl R, Fujita DJ, Jove R, Yeatman TJ. 1999. Activating SRC mutation in a subset of advanced human colon cancers. *Nature Genetics* **21**:187–190. DOI: https://doi.org/10.1038/5971, PMID: 9988270

Kazi JU, Rönnstrand L. 2012. Src-Like adaptor protein (SLAP) binds to the receptor tyrosine kinase Flt3 and modulates receptor stability and downstream signaling. *PLOS ONE* **7**:e53509. DOI: https://doi.org/10.1371/journal.pone.0053509, PMID: 23300935

Kohlmaier A, Fassnacht C, Jin Y, Reuter H, Begum J, Dutta D, Edgar BA. 2015. Src kinase function controls progenitor cell pools during regeneration and tumor onset in the *Drosophila* intestine. *Oncogene* **34**:2371–2384. DOI: https://doi.org/10.1038/onc.2014.163, PMID: 24975577

Leroy C, Fialin C, Sirvent A, Simon V, Urbach S, Poncet J, Robert B, Jouin P, Roche S. 2009. Quantitative phosphoproteomics reveals a cluster of tyrosine kinases that mediates SRC invasive activity in advanced colon carcinoma cells. *Cancer Research* **69**:2279–2286. DOI: https://doi.org/10.1158/0008-5472.CAN-08-2354, PMID: 19276381

Manes G, Bello P, Roche S. 2000. Slap negatively regulates Src mitogenic function but does not revert Src-induced cell morphology changes. *Molecular and Cellular Biology* **20**:3396–3406. DOI: https://doi.org/10.1128/MCB.20.10.3396-3406.2000, PMID: 10779329

Merlos-Suárez A, Barriga FM, Jung P, Iglesias M, Céspedes MV, Rossell D, Sevillano M, Hernando-Momblona X, da Silva-Diz V, Muñoz P, Clevers H, Sancho E, Mangues R, Batlle E. 2011. The intestinal stem cell signature identifies colorectal cancer stem cells and predicts disease relapse. *Cell Stem Cell* **8**:511–524. DOI: https://doi.org/10.1016/j.stem.2011.02.020

Mevizou R, Naim D, Cauchois F, Naudin C, Greaves G, Espie K, Felipe B, Simon V, Boublik Y, Nguyen J, Urbach S, Roche S, Sirvent A. 2026. SLAP controls mTORC2 integrity via UBE3C-mediated non-degradative mLST8 ubiquitination to suppress colorectal tumorigenesis. *Cell Death and Differentiation* **33**:1020–1035. DOI: https://doi.org/10.1038/s41418-025-01633-1, PMID: 41398047

Myers MD, Dragone LL, Weiss A. 2005. Src-like adaptor protein down-regulates T cell receptor (TCR)-CD3 expression by targeting TCRzeta for degradation. *The Journal of Cell Biology* **170**:285–294. DOI: https://doi.org/10.1083/jcb.200501164, PMID: 16027224

Myers MD, Sosinowski T, Dragone LL, White C, Band H, Gu H, Weiss A. 2006. Src-like adaptor protein regulates TCR expression on thymocytes by linking the ubiquitin ligase c-Cbl to the TCR complex. *Nature Immunology* **7**:57–66. DOI: https://doi.org/10.1038/ni1291, PMID: 16327786

Narayanan KK, Amaya M, Tsang N, Yin R, Jays A, Broder CC, Shukla D, Procko E. 2023. Sequence basis for selectivity of ephrin-B2 ligand for Eph receptors and pathogenic henipavirus G glycoproteins. *Journal of Virology* **97**:e0062123. DOI: https://doi.org/10.1128/jvi.00621-23, PMID: 37931130

Naudin C, Sirvent A, Leroy C, Larive R, Simon V, Pannequin J, Bourgaux JF, Pierre J, Robert B, Hollande F, Roche S. 2014. SLAP displays tumour suppressor functions in colorectal cancer via destabilization of the SRC substrate EPHA2. *Nature Communications* **5**:3159. DOI: https://doi.org/10.1038/ncomms4159, PMID: 24457997

Naudin C, Chevalier C, Roche S. 2016. The role of small adaptor proteins in the control of oncogenic signalingr driven by tyrosine kinases in human cancer. *Oncotarget* **7**:11033–11055. DOI: https://doi.org/10.18632/oncotarget.6929, PMID: 26788993

Nguyen J, Lafitte M, Barbery M, Espie K, Jeitany M, Larive R, Vitre J, Paul C, Boublik Y, Fourgous E, Simon V, Sirvent A, Neiveyans M, Thirard S, Bansard L, Maillard M, Coutry N, Colinge J, Jay P, Martineau P, et al. 2025. Progastrin promotes colorectal cancer stem cell-like properties via the receptor PZR. *Advanced Science* **12**:e02136. DOI: https://doi.org/10.1002/advs.202502136, PMID: 40753649

Noberini R, Lamberto I, Pasquale EB. 2012. Targeting Eph receptors with peptides and small molecules: progress and challenges. *Seminars in Cell & Developmental Biology* **23**:51–57. DOI: https://doi.org/10.1016/j.semcdb.2011.10.023

Pandey A, Duan H, Dixit VM. 1995. Characterization of a novel Src-like adapter protein that associates with the Eck receptor tyrosine kinase. *The Journal of Biological Chemistry* **270**:19201–19204. DOI: https://doi.org/10.1074/jbc.270.33.19201, PMID: 7543898

Parseghian CM, Parikh NU, Wu JY, Jiang ZQ, Henderson L, Tian F, Pastor B, Ychou M, Raghav K, Dasari A, Fogelman DR, Katsiampoura AD, Menter DG, Wolff RA, Eng C, Overman MJ, Thierry AR, Gallick GE, Kopetz S. 2017. Dual inhibition of EGFR and c-Src by cetuximab and dasatinib combined with FOLFOX chemotherapy in patients with metastatic colorectal cancer. *Clinical Cancer Research* **23**:4146–4154. DOI: https://doi.org/10.1158/1078-0432.CCR-16-3138, PMID: 28280091

Pasquale EB. 2024. Eph receptor signaling complexes in the plasma membrane. *Trends in Biochemical Sciences* **49**:1079–1096. DOI: https://doi.org/10.1016/j.tibs.2024.10.002, PMID: 39537538

Paul C, Tang R, Longobardi C, Lattanzio R, Eguether T, Turali H, Bremond J, Maurizy C, Gabola M, Poupeau S, Turtoi A, Denicolai E, Cufaro MC, Svrcek M, Seksik P, Castronovo V, Delvenne P, de Laurenzi V, Da Costa Q, Bertucci F, et al. 2022. Loss of primary cilia promotes inflammation and carcinogenesis. *EMBO Reports* **23**:e55687. DOI: https://doi.org/10.15252/embr.202255687, PMID: 36281991

Reddy SM, Kopetz S, Morris J, Parikh N, Qiao W, Overman MJ, Fogelman D, Shureiqi I, Jacobs C, Malik Z, Jimenez CA, Wolff RA, Abbruzzese JL, Gallick G, Eng C. 2015. Phase II study of saracatinib (AZD0530) in patients with previously treated metastatic colorectal cancer. *Investigational New Drugs* **33**:977–984. DOI: https://doi.org/10.1007/s10637-015-0257-z, PMID: 26062928

Roche S, Alonso G, Kazlauskas A, Dixit VM, Courtneidge SA, Pandey A. 1998. Src-like adaptor protein (Slap) is a negative regulator of mitogenesis. *Current Biology* **8**:975–978. DOI: https://doi.org/10.1016/s0960-9822(98)70400-2, PMID: 9742401

Sirvent A, Leroy C, Boureux A, Simon V, Roche S. 2008. The Src-like adaptor protein regulates PDGF-induced actin dorsal ruffles in a c-Cbl-dependent manner. *Oncogene* **27**:3494–3500. DOI: https://doi.org/10.1038/sj.onc.1211011, PMID: 18193084

Sirvent A, Benistant C, Roche S. 2012. Oncogenic signaling by tyrosine kinases of the SRC family in advanced colorectal cancer. *American Journal of Cancer Research* **2**:357–371 PMID: 22860228.

Sirvent A, Mevizou R, Naim D, Lafitte M, Roche S. 2020. Src family tyrosine kinases in intestinal homeostasis, regeneration and tumorigenesis. *Cancers* **12**:2014. DOI: https://doi.org/10.3390/cancers12082014, PMID: 32717909

Sosinowski T, Killeen N, Weiss A. 2001. The Src-like adaptor protein downregulates the T cell receptor on CD4+CD8+ thymocytes and regulates positive selection. *Immunity* **15**:457–466. DOI: https://doi.org/10.1016/s1074-7613(01)00195-9, PMID: 11567635

Summy JM, Gallick GE. 2003. Src family kinases in tumor progression and metastasis. *Cancer Metastasis Reviews* **22**:337–358. DOI: https://doi.org/10.1023/a:1023772912750, PMID: 12884910

Takahashi M, Wakabayashi K. 2004. Gene mutations and altered gene expression in azoxymethane-induced colon carcinogenesis in rodents. *Cancer Science* **95**:475–480. DOI: https://doi.org/10.1111/j.1349-7006.2004.tb03235.x, PMID: 15182426

Tang Z, Kang B, Li C, Chen T, Zhang Z. 2019. GEPIA2: an enhanced web server for large-scale expression profiling and interactive analysis. *Nucleic Acids Research* **47**:W556–W560. DOI: https://doi.org/10.1093/nar/gkz430

Wong VWY, Stange DE, Page ME, Buczacki S, Wabik A, Itami S, van de Wetering M, Poulsom R, Wright NA, Trotter MWB, Watt FM, Winton DJ, Clevers H, Jensen KB. 2012. Lrig1 controls intestinal stem-cell homeostasis by negative regulation of ErbB signalling. *Nature Cell Biology* **14**:401–408. DOI: https://doi.org/10.1038/ncb2464

Wybenga-Groot LE, McGlade CJ. 2015. RTK SLAP down: the emerging role of Src-like adaptor protein as a key player in receptor tyrosine kinase signaling. *Cellular Signalling* **27**:267–274. DOI: https://doi.org/10.1016/j.cellsig.2014.11.010, PMID: 25446260

Yang M, Davis TB, Pflieger L, Nebozhyn MV, Loboda A, Wang H, Schell MJ, Thota R, Pledger WJ, Yeatman TJ. 2022. An integrative gene expression signature analysis identifies CMS4 KRAS-mutated colorectal cancers sensitive to combined MEK and SRC targeted therapy. *BMC Cancer* **22**:256. DOI: https://doi.org/10.1186/s12885-022-09344-3, PMID: 35272617

Zhang S, Kutibiding A, Wang M, Zhou X, Tian X, Liu D, Manafu T, Li R, Guo H, Zhao W, Yang Y. 2026. M2 macrophage-derived migrasomes orchestrate dual CXCL12/CXCR4 and neutrophil-MMP-9/MSC-EphB2 signaling to enhance fracture healing. *Cell Biomaterials* **2**:100258. DOI: https://doi.org/10.1016/j.celbio.2025.100258

Zisch AH, Kalo MS, Chong LD, Pasquale EB. 1998. Complex formation between EphB2 and Src requires phosphorylation of tyrosine 611 in the EphB2 juxtamembrane region. *Oncogene* **16**:2657–2670. DOI: https://doi.org/10.1038/sj.onc.1201823, PMID: 9632142

Zutshi N, Mohapatra BC, Mondal P, An W, Goetz BT, Wang S, Li S, Storck MD, Mercer DF, Black AR, Thayer SP, Black JD, Lin C, Band V, Band H. 2024. Cbl and Cbl-b ubiquitin ligases are essential for intestinal epithelial stem cell maintenance. *iScience* **27**:109912. DOI: https://doi.org/10.1016/j.isci.2024.109912